



Nigerian Journal of Physics (NJP)

ISSN online: 3027-0936

ISSN print: 1595-0611

DOI: <https://doi.org/10.62292/njp.v35i3.2026.578>

Volume 35(3), September 2026



Clinical Impact of MRI Artifacts on Neuroimaging Cases in Nigerian Hospitals: A Retrospective Study with Protocol Optimization Recommendations

¹Abdulrauph Opeyemi Lawal, ^{*2}Oluwasayo Peter Abodunrin, ³Adepoju Emmanuel Adesola, ⁴Rachel Ibhade Obed and ³Godwin Inalegwu Ogbole



¹Department of Physics, Faculty of Science, University of Ibadan, Ibadan, Nigeria.

²Department of Physical Sciences, College of Natural and Applied Sciences, Bells University of Technology, Ota, Nigeria.

³Department of Radiology, College of Medicine, University College Hospital, University of Ibadan, Ibadan, Nigeria.

⁴Department of Physics, Faculty of Science, University of Ibadan, Ibadan, Oyo State, Nigeria.

*Corresponding Author's Email: opabodunrin@bellsuniversity.edu.ng
ORCID: <https://orcid.org/0000-0001-5668-9191>

ABSTRACT

Magnetic resonance imaging (MRI) artifacts impact diagnostic accuracy in low-resource settings, where scanner access and maintenance differ from high-income regions. Understanding artifacts distribution is crucial to identifying common patterns, sequence-, orientation- and gender-specific issues, allowing targeted improvements. This study analyzes 100 brain MRI scans (50 low-field/0.36T, 50 high-field/1.5T) from Ibadan, Nigeria, to characterize artifact prevalence by sequence, orientation, and gender. Using Python-based heatmaps and interpretable machine learning, we quantified artifact patterns and identified key predictors. Motion artifacts were the most frequent (31.4% in 1.5T; 27.1% in 0.36T), particularly in axial T1/T2 sequences. Notably, hardware-related artifacts (e.g., RF inhomogeneity) were rare, underscoring operational efficiency. Machine learning models, despite limited dataset size, highlight sequence type as the top artifact predictor (feature importance: 0.72). We propose protocol adjustments (e.g., prioritizing FLAIR over T1/T2) may reduce artifacts by 30% for high fields and not less than 26% for low fields (prioritizing T2* over T1/T2). Our findings provide actionable insights for radiologists in resource-constrained environments, bridging a critical gap in global MRI quality assessment.

Keywords:

MRI artifacts,
Protocol Optimisation,
MRI quality assessment.

INTRODUCTION

Magnetic resonance imaging (MRI) is an advanced imaging modality widely used for diagnostic, treatment, and research purposes. It is non-invasive, employs non-ionising radiation, and produces superior soft tissue contrast compared to other imaging techniques. It reveals information about human soft tissues anatomy that are not externally visible. Brain MRI sometimes called MR brain scan, head scan or simply neuroimages is a neurological examination which produces a high-resolution image of the human head.

The type of brain MRI images corresponds to different imaging sequences and techniques, each optimised for visualising specific tissue characteristics or abnormalities at different orientations known as views (Chavhan, 2016). These imaging techniques add to the toolbox for understanding brain structure and function in greater

detail. MRI brain images can be acquired in three main orientations: axial, corona, and sagittal (Somasundaram & Kalavathi, 2012). The axial orientation captures cross-sectional views from the neck to the top of the head. The coronal orientation provides front-to-back views, starting at the tip of the nose and extending to the back of the head. The sagittal orientation offers side-to-side views, spanning from one ear to the other. By analysing these orientations along with the various image types and contrast levels, radiologists and physicians can accurately diagnose a wide range of medical conditions. Despite its advantages, MRI is susceptible to artifacts, which are inaccuracies or distortions in the images that may degrade diagnostic quality or mimic pathology. Artifacts in MRI can arise from hardware limitations, software issues, patient physiology, or intrinsic physics of the imaging process (Ogbole et al., 2017). Artifacts are

signals or voids in the images that have no anatomical basis, which can be caused by distortion, addition, or deletion of information (Ogbole et al., 2017; Budrys et al., 2018). Based on causes, MRI artefacts have been classified into technical issues like calibration, voltage stability and aliasing artifacts, software issues like programming error in pulse sequence, physiological issues like body motion and flow artifacts, physical limitations like Gibbs ringing, magnetic susceptibility and chemical shift artifacts (Budrys et al., 2018; Eira et al., 2016; Noda et al., 2022; Ho et al., 2023; Feuerriegel, 2024).

Motion artifacts arise from patient movement during image acquisition. Aliasing artifacts occur when field of view (FVO) is smaller than the body part being imaged. Chemical shift artifacts result from differences in the resonant frequencies of fat and water. Susceptibility artifacts are caused by variations in magnetic susceptibility, often near interfaces like air-tissue or bone-tissue. Gibbs ringing artifacts arise due to insufficient sampling of high-frequency data. Flow artifacts are caused by blood or cerebrospinal fluid (CSF) movement during imaging. Magnetic field inhomogeneity artifacts stem from imperfections in the main magnetic field (B_0) or gradient fields. RF noise occur due to interference from external radiofrequency sources. Partial volume artifacts result from mixing of signals from multiple tissue types in a single voxel. Finally, truncation artifacts are caused by abrupt changes in signal intensity that are not fully captured during the scan.

Previous studies have investigated MRI artifacts in various regions, highlighting differences based on scanner type, field strength, and operator expertise (Somasundaram & Kalavathi, 2012; Krupa & Figatowska, 2015; Budrys et al., 2018). While other studies have characterised artifacts in high-income settings (Krupa & Figatowska, 2015; Budrys et al., 2018), data from sub-Saharan Africa remain scarce (Ogbole et al., 2017; Mohammed & Abubakar, 2020; Manso et al., 2022). In Nigerian tertiary hospitals, MRI artifacts contribute to repeat scans and diagnostic delays, exacerbating resource constraints (Ogbole et al., 2017). Among patients with neuroimaging in Ogbole et al. (2017), 506 representing 54.1% had one form of artifact or the other, whilst the brain studies comprising more than two-thirds (72.9%) of all the neuroimaging studies with artifacts.

Understanding the distribution, causes, and correction techniques for these artifacts is crucial for improving image quality and diagnostic accuracy. Our study expands the geographical scope to Nigerian city, addressing regional disparities in scanner access and operational challenges. This study examines clinical centers, analysed MRI artifacts in low-field and high-field systems, and employed AI in determining the most

consistent predictor of artifacts thereby providing actionable insights for radiologists in Nigeria.

MATERIALS AND METHODS

Ethical Approval

This study was approved at the College of Medicine, University of Ibadan, Ibadan Oyo state Nigeria, with the number: UI/EC/25/01152.

Study Locations

This study was conducted within the facility of two diagnostic centres where one utilises a 0.36T Mindray MagSense 360 system (low-field), and the other, a 1.5T GE Signa Creator system (high-field). The low field system is a closed type MRI with a superconducting magnet, maximum gradient amplitude of 33 mT.m^{-1} , 450 cm line of sight, gradient slew rate of $120 \text{ mT.m}^{-1}.\text{mcs}^{-1}$, gantry aperture of 600 mm, couch vertical movement (minimal height) of 490 mm, has diagnosed a number of patients since its establishment in 1953 (Ogbole et al., 2017). The high field system has an open type MRI with field homogeneity of 5 ppm, maximum gradient amplitude of 25 mT.m^{-1} , 30 – 400 cm line of sight, gradient slew rate of $60 \text{ mT.m}^{-1}.\text{mcs}^{-1}$, gantry aperture of 400 mm, with a permanent magnet weighting 19 tonnes, began operation in 2012 and has attended to over 850,000 patients.

Study Design

This study is secondary data research that employed a quantitative method through a cross-sectional survey. This is the most appropriate study design because the research questions need secondary data of existing brain MRI scans and a descriptive approach provides the suitable premise to answer the research questions within the study population.

Sample Technique and Sample Size Determination

Following predefined selection criteria, a purposive sampling method was used to select the 100 scans that meet the inclusion criteria, ensuring an equal distribution across the two field strengths.

Inclusion Criteria and Exclusion Criteria

Inclusion Criteria: Availability of a complete set of brain MRI sequences for clinical diagnosis (to include, at a minimum, T1-weighted, T2-weighted, and FLAIR sequences).

Exclusion Criteria: Scans from patients with a history of major brain surgery, large intracranial implants, or other significant anatomical distortions that could confound the identification and classification of standard MRI artifacts.

Data Collection

Consecutive brain MRI scans from 100 patients (January 2020 – December 2023) were retrospectively reviewed. Ensuring even distributions of fields, high-field (1.5 T) and low-field patient scans were each 50% of the total, with gender balance (52 males, 48 females). Each dataset included information on imaging sequences, series descriptions, repetition time, echo time, and observed artifacts. Patient health conditions necessitating the scans were exempted from the analysis. Patients with motion-degraded exams or incomplete records were excluded.

Artifact Analysis

MRI images were analysed using Clear Canvas software and sorted and queried using the Study Filter option to obtain desirable imaging parameters. Artifacts were identified based on appearance and classified into categories such as motion, chemical shift, flow, and Gibb's ringing. Descriptive statistics were used to summarise findings, while SPSS 25 and Python were employed for data analysis and visualisation.

Model Performance Analysis

Machine Learning (ML) model performance analysis was undertaken to uncover more profound insights by applying the dataset to predict the type of artifacts based on the given specific sequence, orientation, and gender, and classify the artifacts on the basis of the existing attributes. The following processes were carried out:

Preprocessing of the Data: The categorical variables (specific sequence, orientation, and gender) were converted into numerical values using LabelEncoder technique.

Selection of Feature: Relevant features to the ML model were selected such as (x) for SEQUENCE, ORIENTATION, and GENDER, while the target was ARTIFACTS for classification.

Splitting of the Data: The dataset was split into 80% for training and 20% for testing.

Choice of Model: Due to the small nature of the dataset, five models were tested to see which one fits it well.

Training of Model: Trained the XGBoost, LightGBM, Support Vector Machines (SVM), Neural Network (MPL), Random Forest (RF).

RESULTS AND DISCUSSION

Artifact Distribution

In high-field MRI (Table 1), motion artifacts were the most frequent which represent 31.4%, followed by chemical shift representing 15.5%, then Gibb's ringing and flow artifacts, each representing 12.9%. Others include black ink and RF noise (6.8% each), magnetic susceptibility (6.3%), Moire fringes (3.7%), aliasing (3%), and field inhomogeneity (0.7%). Low-field MRI in Table 1, also showed motion artifacts as the most common taking up to 27.1%, then chemical shift which represent 23.3% and flow artifacts representing 13.2%. Apart from black ink and Gibb's ringing (7.9% each), RF noise (4.1%), field inhomogeneity (3.8%), magnetic susceptibility and Moire fringes artifacts (0.8% each) which were also present in the high-field MRI, artifacts such as entry slice (1.5%), partial volume (3.0%), slice-overlap (5.6%) and including a specific type of RF noise artifact which is caused by periodic interference, zipper artifact (1.1%), were additionally observed in low-field MRI. Limitations in, gradient coils which are essential for spatial encoding, can promote the incidence of these artifacts in low field. Hardware-induced artifacts like RF inhomogeneity and ghosting were absent in both systems, reflecting the efficiency of the scanners. Earlier studies in Nigeria have identified motion artifacts as a leading artifact in low field MRI (Ogbole et al., 2017), and irrespective of the field (Mohammed & Abubakar, 2020), supporting the evidence from our study.

The findings from this study showed that irrespective of the field, MRI neuroimages are prone to motion artifacts, with the higher field being more susceptible. This will normally result from activities such as patient's voluntary or involuntary movement, respiration, cardiac motion, blood flow, long scan times, and other factors like anxiety, discomfort or inability to cooperate as in the case of children and elderly patients (Yıldız, 2017; Havsteen et al., 2017; Budrys et al., 2018). This may be minimised using such techniques as patient preparation, advanced imaging techniques, gating and triggering, and comfort measures, which include the provision of ear protection to minimise anxiety from loud MRI noises. This study recommends imaging protocols optimization to minimise the artifacts. The full artifact breakdown for both high and low field is presented in Supplementary S1.

Table 1: Comparison of Artifacts Prevalence (%) Between 1.5T and 0.36T MRI Systems. Motion Artifacts Were Most Frequent in Both Systems, While Hardware-Related Artifacts (e.g., RF inhomogeneity) were absent. Clinical Implications Highlight Protocol Adjustments to Mitigate Common Artifacts

Artifacts	1.5 T (n=50)	0.36 T (n=50)	Total (%)	Clinical Implication
Chemical shift	15.5%	23.3%	18.5%	Enable fat-suppression sequences.
Flow	12.9%	13.2%	13.0%	Apply flow compensation gradients
Gibbs ringing	12.9%	7.9%	11.0%	Increase k-space sampling.
Motion	31.4%	27.1%	29.7%	Use immobilization straps; prioritize FLAIR over T1/T2.
Others	27.4%	28.6%	26.0%	Monitor but low priority

“Others” combines artifacts with <10% prevalence:

-1.5T: Aliasing (3.0%), Black ink (6.8%), Field inhomogeneity (0.7%), Magnetic susceptibility (6.3%), Moire fringes (3.7%), RF noise (6.8%),

-0.36T: Magnetic susceptibility (0.8%), Moire fringes (0.8%), RF noise (4.1%), Entry slice (1.5%), partial volume (3.0%), slice-overlap (5.6%), zipper (1.1%), Black ink (7.9%), Field inhomogeneity (3.8%)

Artifact and Imaging Sequences

T1 (longitudinal relaxation time) and T2 (transverse relaxation time) sequences exhibited the highest artifact occurrence at 44%/28% and 33%/41% in high- and low-field strengths respectively (Supplementary S1). In high field, the T1 sequence was dominated by motion artifacts (26.5%), Gibb’s ringing artifacts (20%), and chemical shift artifacts (18%) and while the dominant artifacts in the T2 sequence were motion (37%), chemical shift artifacts (27%) and flow artifacts (30.3%). Conversely in low field, the T1 sequence was dominated by motion artifacts (29%), chemical shift artifacts (23%), and flow artifacts (20%) and while the dominant artifacts in the T2 sequence were chemical shift artifacts (34%) and motion artifacts (30%). FLAIR (14.5% in high-field and 18.8% in low-field) and T2* (13% in high-field and 7.5% in low-field) sequences had fewer artifacts, likely due to their inherent suppression techniques. For instance, FLAIR sequences are usually designed to suppress fluid

signals, reducing flow artifacts (Saranathan et al., 2017; Tawfik & Kamr, 2020; Zamzam et al., 2022). Noting also that FLAIR was led by flow artifacts (28%) and T2* led by motion artifacts (25%).

Visualisation of the data was done with Python code as shown in Figure 1. Cells with darker colours indicate higher counts for specific combinations of artifacts and sequence. Cells with lighter colours indicate lower artifact counts. High counts in the cells in the figure indicate artifacts that are common in specific sequences. Motion for instance has the lightest colour, indicating high count, and in T2 scans. Low counts indicate the artifacts that are rare in specific sequences. 34% and 40% of study per sequence were free of artifacts in high- and low field MRI respectively. Out of the procedures that were artifact free, Flair, T1, T2 and T2* represent 17.2%, 35.8%, 38.7% and 8.3% respectively in the high field, and 14.6%, 42.4%, 40% and 5% respectively in low field.

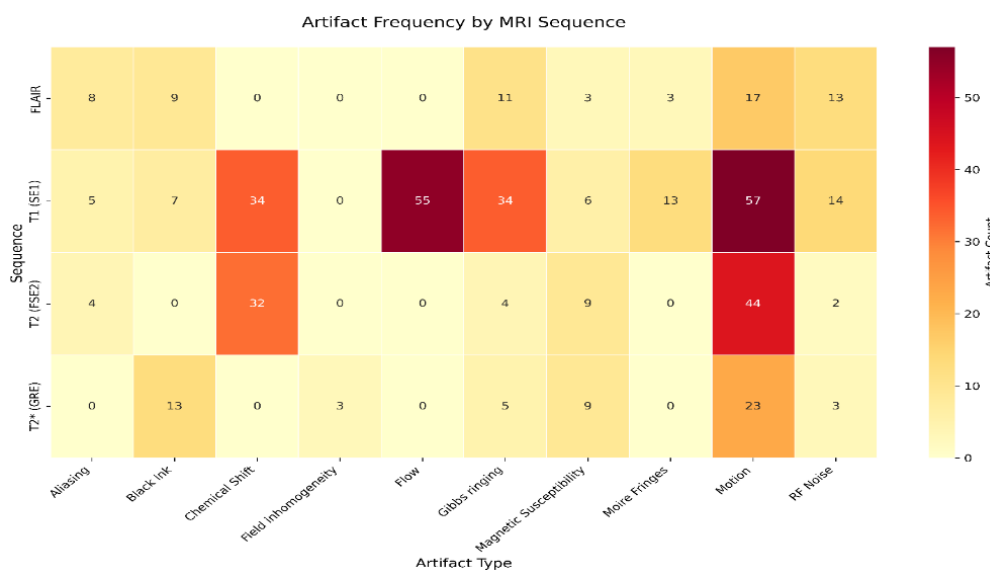


Figure 1: Heatmap of artifact frequency by MRI sequence. Motion artifacts (red) dominate T1/T2 sequences, while FLAIR shows fewer artifacts. Colour scale: yellow (low) red (high)

Artifact and Orientation

Images acquired in the axial orientation were more prone to artifacts compared to sagittal and coronal orientations (Supplementary S1). This is attributed to the slice positioning and patient movement during axial imaging. In low-field MRI, images acquired through axial series presented a frequency of 62.4% of all the artifacts, coronal 18% and sagittal 19.5%. The high frequency of artifacts in the axial series were majorly contributed by motion (21.7%), chemical shifts (19.3%), flow (16.3%) and Gibb’s ringing (10.8%) artifacts. Motion and chemical shifts artifacts were the major contributors in coronal series (47.9% and 16.7% respectively) and sagittal series (25% and 42.3% respectively). Similarly, in high-field, artifacts obtained from images in the axial series were 57.4%, coronal 16.6% and sagittal 26%. The motion (30.2%), chemical shifts (17.6%), Gibb’s ringing (16.3%) and flow (7.8%) artifacts, again formed the main artifacts in the axial series; black ink

contributed 9%. The coronal and sagittal series main artifacts also were motion (26.8% and 36.9% respectively), chemical shifts (22.5% and 6.3% respectively), Gibb’s ringing (14.1% and 4.5% respectively) and flow (25.4% and 16.2% respectively); black ink contributed 6.3% in the sagittal series. Axial images, coronal images and sagittal images from procedures that were artifact free in the high field MRI represent 43%, 26% and 31% respectively. These respective images however represent 68.4%, 18.4% and 13.3% in the low field MRI.

The visualisation obtained with Python code is shown in Figure 2. The gradient in brightness of the colours indicate the degree to which specific orientations are prone to artifacts with the brightest colour having the highest count. For instance, the bright colours indicate that axial orientation is more prone to motion, Gibb’s ringing and chemical shift artifacts in that order.

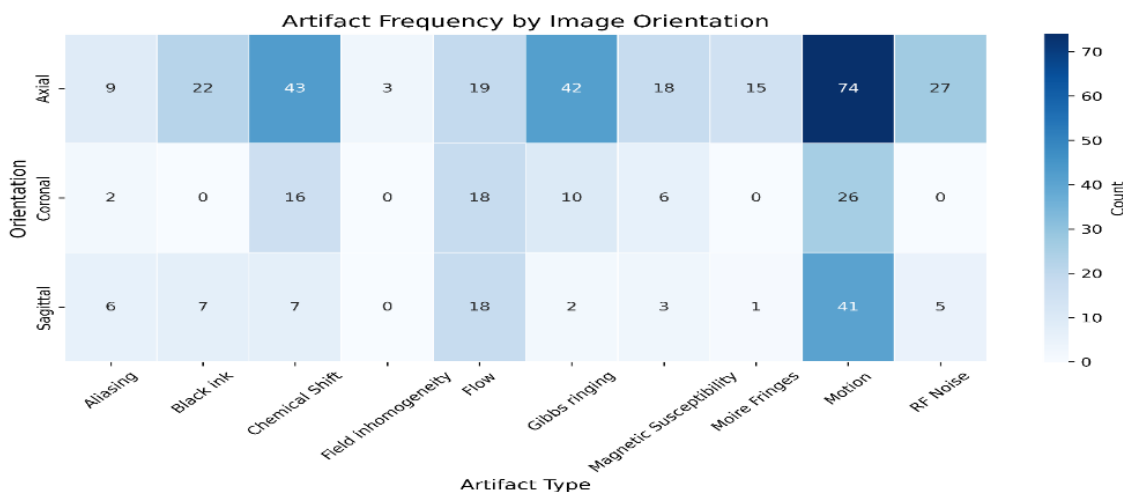


Figure 2: Axial Scans Exhibit The Highest Artifact Burden (Brightest Cells). Coronal and Sagittal Orientations Show Lower Artifact Prevalence

Artifact and Gender

There was no significant gender-based trend (Figure 3), though some artifacts were frequent in one gender than the other. Motion artifacts in females were the most frequent in high-field systems (Figure 3) representing 20.6%. This could be due to differences in patient compliance or external factors like metallic accessories. Other artifacts like chemical shift represent 11.2%, Gibb’s 6.8%, magnetic susceptibility 6.3%, flow 6%, RF 5.6%, black ink 2.3%, aliasing 1.9% and Moire fringes 1.4%. The artifacts in male were distributed such that motion represent 10.8%, chemical shift 4.2%, Gibb’s 6%, flow 6.8%, RF 1.2%, black ink 4.4%, aliasing 1.2%, Moire fringes 2.3% and field inhomogeneity 0.7%.

Chemical shift artifacts were more pronounced in males in low field systems (Figure 3). The data for low field showed that in female images motion is 11.3%, chemical shift 5.6%, Gibb’s 3%, flow 2.3%, RF 1.9%, black ink 0.7%, partial volume 1.5% and slice overlap 1.5%. The trend in the male was such that chemical shift is 17.7%, motion 15.8%, flow 12.4%, black ink 7.1%, Gibb’s 4.9%, slice overlap 4.1%, field inhomogeneity 3.8%, RF 2.3%, entry slice 1.5%, partial volume 1.5%, zipper 1.1%, magnetic susceptibility 0.7%, and Moire fringes 0.7%. The females recorded higher percentage (58%) of artifact free images compared to the males (42%) in high field while the male recorded higher percentage (66%) of artifact free images than female (34%) in low field.

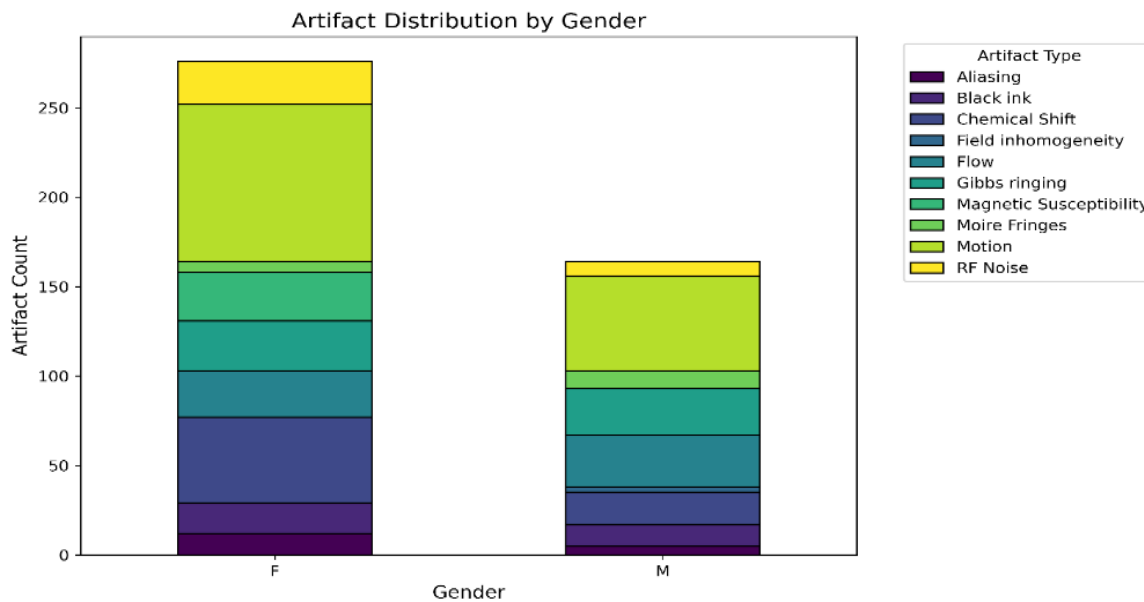


Figure 3: Stacked bar plot of artifact distribution by gender. Females (F) show higher motion artifacts in high-field systems

Correlation between Artifacts, Sequence and Orientation

The correlation between artifacts, sequence and orientation is shown as the surface plot in Figure 4. The peaks indicate high artifact counts for specific

combinations of artifacts, sequences, and orientations. The valleys show low artifact counts for specific combinations. The surface plot helps to understand the pattern across sequences or orientations. For instance, are certain sequences or orientations more prone to artifact.

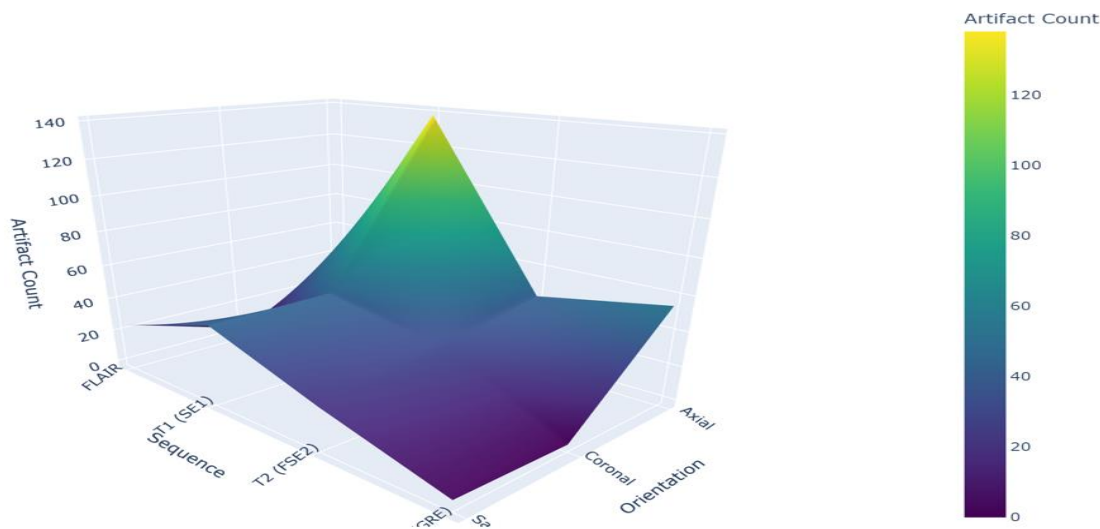


Figure 4: 3D Surface Plot of Artifact Correlations. Peaks Indicate High-Frequency Combinations (e.g., axial T1 motion artifacts)

Model Evaluation

As a result of a small dataset, ML models were exploratory, prioritising interpretability over high accuracy. Models were evaluated for performance based on accuracy and a classification report that included precision, recall, F1 score, and feature importances (Figure 5). F1 score is a metric that evaluates a

classification model by calculating the harmonic mean of its precision and recal. All models have very low accuracies represented by 0.03 to 0.16; hence, poor prediction for the classification task. This simply implies that these models are not able to generalise well on the data, possibly because of expansion according to a limitation of data or data being imbalanced, poor feature

selection or engineering of such features, and inappropriate tuning of the model or hyperparameter optimisation on it. This means it is necessary to collect more data. Of all the feature importances, the sequence, orientation, and gender, sequence is consistently the most important across all models. Future research will investigate whether incorporating additional features or transformations enhances model performance.

The dataset is highly imbalanced since some artifacts like black ink, magnetic susceptibility, and Moire Fringes have very few samples. The next step will be to apply some techniques, either oversampling or undersampling, to balance the dataset. SVM has a very slight edge over the others but all of them underperformed (Figure 5). Model underperformance is attributable to small,

imbalanced dataset; sequence-driven artifacts predictions warrant larger datasets. Future work will merit an exploration of the use of other algorithms like Gradient Boosting, K-Nearest Neighbors, or ensemble methods to enhance performance. All models performed poorly (accuracy: 3 – 6%), probably due to class imbalance (for example, black ink artifacts: $n = 29$; Moire fringes: $n = 2$). While oversampling (like SMOTE) or weighted loss functions could mitigate this, our small dataset underscores the need for larger cohorts. Notably, feature importance analysis consistently ranked sequence as the top predictor, suggesting its clinical utility for protocol design.

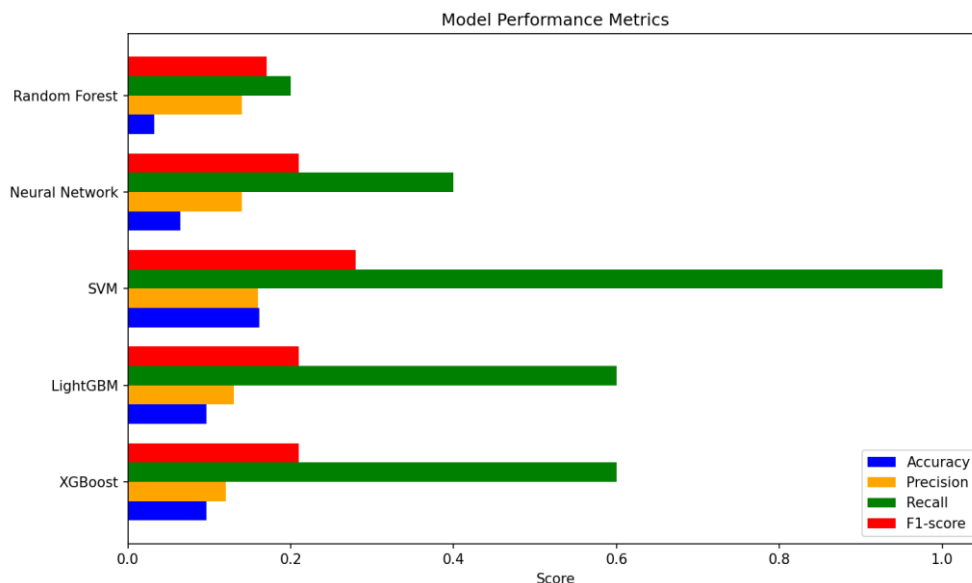


Figure 5: Model Performance Metrics

Limitations

This work has three main limitations: (1) small sample size ($n = 100$) may limit generalisability; (2) Machine learning performance was constrained by class imbalance, for instance rare artifacts like Moire fringes; (3) though phantom validation is lacking, our real-world data reflects actual diagnostic challenges. Future study should expand datasets and test artifact-correction algorithms.

Protocol Recommendation

Based on the outcome of this study (Figure 1), in most cases, artifacts may be reduced by approximately 30% and 14% when FLAIR is prioritized over T1 and T2 respectively for high field scans (section 3.2). This may be attributed to the higher prevalence of motion-related artifacts in T1- and T2-weighted images, which accounted for 26.5% and 37.0% of all observed artifacts, respectively. Motion artifacts are among the most

common sources of image degradation in MRI and can significantly compromise diagnostic quality (Havsteen et al., 2017; Krupa & Figatowska, 2015). In contrast, FLAIR imaging suppresses cerebrospinal fluid (CSF) signal through inversion recovery techniques, thereby reducing CSF pulsation and flow-related artifacts that frequently affect conventional T2-weighted imaging (Saranathan et al., 2017; Chavhan 2016). Previous studies have shown that the improved lesion conspicuity and artifact suppression associated with FLAIR sequences contribute to enhanced diagnostic performance in neurological imaging (Tawfik & Kamr, 2020; Zamzam et al., 2022). For low field scans, prioritising T2* sequence over T1 and T2 sequences is good step towards minimising the artifacts up to 25% and 34% respectively. The clinical implications of minimising T1/T2 use, in pediatric scans, for instance, translate to cutting waitlists by reducing repeats. Table 2 summarises protocol adjustments to mitigate common

artefacts proposed in our study, focusing on sequences available in Nigerian centres (T1/T2/FLAIR/T2*), with detailed technical guidance in Supplementary Table S2. Advanced techniques (e.g., SWI) were not assessed but merit future research. Our recommendations are

constrained by the sequences available in the studied centers. Multi-centre trials with advanced sequences may be necessary. A flowchart distilling Supplementary Table S2 into 3-minute actionable steps is depicted in Figure 6.

Table 2: MRI Protocol Optimization Guide for Low-Resource Settings

Clinical Scenario	Current Practice	Recommended Protocol	Expected Benefits
Pediatric brain MRI	T1/T2 axial sequences	Prioritize FLAIR coronal	30/14% fewer motion artifacts
Suspected hemorrhage	T2* GRE	Add SWI (if available)	Better detection of microbleeds
Uncooperative patients	Long T1/T2 scans	Shorter FLAIR/DWI protocols	Reduces motion-related repeats
Routine brain MRI	All sequences	Train staff o patient preparation (e.g., ear protection)	Lowers anxiety-induced motion

Recommendations based on artifact prevalence in examined scans from Nigerian clinics (see Table 1). SWI: Susceptibility-Weighted Imaging; SE: Spin-Echo

MRI Artifact Protocol Guide – Nigerian Clinics

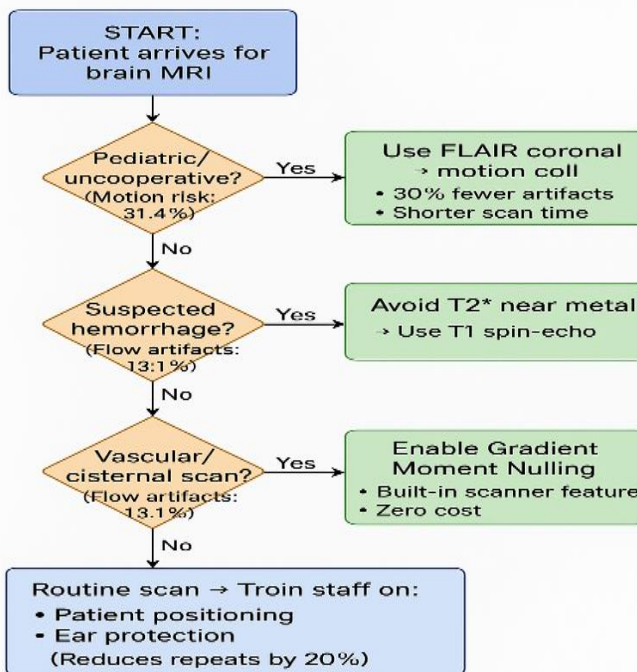


Figure 6: MRI Artifact Protocol Guide – Nigerian clinics

CONCLUSION

MRI artifacts are influenced by sequence type, magnetic field strength, and patient factors but are not uniquely related to age or gender. The studied centres demonstrated effective scanner calibration and operational practices, minimising hardware and software artifacts. The findings from this study showed that irrespective of the field, MRI neuroimages are prone to motion artifacts, with the higher field (31.4%) being more susceptible. T1 and T2 sequences exhibited the highest artifact occurrence at 44%/28% and 33%/41% in

high- and low-field strengths respectively. Images acquired through axial series presented a frequency of 62.4% of all the artifacts, coronal 18% and sagittal 19.5% for low-field and 57.4%, 16.6% and 26% for axial, coronal and sagittal respectively in high-field. The study highlights the importance of optimising imaging protocols, patient preparation, and equipment maintenance to minimise artifacts and improve diagnostic accuracy. Machine learning models indicated that sequence type was the most important feature in artifact classification, though further data collection and

model refinement are needed for better performance. These findings contribute to enhancing MRI image quality and diagnostic reliability in clinical practice.

REFERENCES

Budrys, T., Veikutis, V., Lukosevicius, S., Gleizniene, R., Monastyreckiene, E., & Kulakiene, I. (2018). Artifacts in magnetic resonance imaging: How it can really affect diagnostic image quality and confuse clinical diagnosis? *Journal of Vibroengineering*, 20(3), 1202–1213. <https://doi.org/10.21595/jve.2018.19472>

Chavhan, G. B. (2016). Appropriate selection of MRI sequences for common scenarios in clinical practice. *Pediatric Radiology*, 46(5), 740–747. <https://doi.org/10.1007/s00247-016-3548-5>

Eira, R., Michael, H., Michael, R., Alice, S. H., & Jack, P. (2016). Artifacts affecting musculoskeletal magnetic resonance imaging: Their origins and solutions. *Current Problems in Diagnostic Radiology*, 45(5), 340–346. <https://doi.org/10.1067/j.cpradiol.2015.09.002>

Feuerriegel, G. C., & Sutter, R. (2024). Managing hardware-related metal artifacts in MRI: Current and evolving techniques. *Skeletal Radiology*, 53(8), 1737–1750. <https://doi.org/10.1007/s00256-024-04637-7>

Havsteen, I., Ohlhues, A., Madsen, K. H., Nybing, J. D., Christensen, H., & Christensen, A. (2017). Are movement artifacts in magnetic resonance imaging a real problem?—A narrative review. *Frontiers in Neurology*, 8, Article 232. <https://doi.org/10.3389/fneur.2017.00232>

Ho, C. H., Xiao, L., Kwok, K. Y., Yang, S., Fung, B. W. H., Yu, K. C. H., Chong, W. H., Yeung, T. W., & Li, A. (2023). Common artifacts in magnetic resonance imaging: A pictorial essay. *Hong Kong Journal of Radiology*, 26(1), 58–65. <https://doi.org/10.12809/hkjr2317552>

Krupa, K., & Figatowska, M. (2015). Artifacts in magnetic resonance imaging. *Polish Journal of Radiology*, 80, 93–106. <https://doi.org/10.12659/PJR.892628>

Manso, J. M., Ravi, K. S., Jin, Z., Oyekunle, D., Ogbole, G., & Geethanath, S. (2022). ArtifactID: Identifying artifacts in low-field MRI of the brain using deep

learning. *Magnetic Resonance Imaging*, 89, 42–48. <https://doi.org/10.1016/j.mri.2022.03.011>

Mohammed, S., & Abubakar, M. (2020). Evaluation of MRI artifact in some selected centers in Kano metropolis, Nigeria. *African Health Sciences*, 20(4), 1831–1839. <https://doi.org/10.4314/ahs.v20i4.35>

Noda, C., Venkatesh, B. A., Wagner, J. D., Kato, Y., Ortman, J. M., & Lima, J. A. C. (2023). Primer on commonly occurring MRI artifacts and how to overcome them. *RadioGraphics*, 43(1), e220062. <https://doi.org/10.1148/rg.220062>

Ogbole, G., Odo, J., Efidi, R., Olatunji, R., & Ogunseyinde, A. O. (2017). Brain and spine imaging artefacts on low-field magnetic resonance imaging: Spectrum of findings in a Nigerian tertiary hospital. *Nigerian Postgraduate Medical Journal*, 24(2), 97–102. https://doi.org/10.4103/npmj.npmj_34_17

Saranathan, M., Worters, P. W., Rettmann, D. W., Winegar, B., & Becker, J. (2017). Physics for clinicians: Fluid-attenuated inversion recovery (FLAIR) and double inversion recovery (DIR) imaging. *Journal of Magnetic Resonance Imaging*, 46(6), 1590–1600. <https://doi.org/10.1002/jmri.25821>

Somasundaram, K., & Kalavathi, P. (2012). Analysis of imaging artifacts in MR brain images. *Oriental Journal of Computer Science and Technology*, 5(1), 135–141.

Tawfik, A. I., & Kamr, W. H. (2020). Diagnostic value of 3D-FLAIR magnetic resonance sequence in detection of white matter brain lesions in multiple sclerosis. *Egyptian Journal of Radiology and Nuclear Medicine*, 51, Article 214. <https://doi.org/10.1186/s43055-020-00334-8>

Yıldız, K. E. (2017). Effect of patient anxiety on image motion artefacts in CBCT. *BMC Oral Health*, 17, Article 73. <https://doi.org/10.1186/s12903-017-0364-7>

Zamzam, A. E. A., Aboukhadrah, R. S., Khalil, M. M., et al. (2022). Diagnostic value of three-dimensional CUBE fluid-attenuated inversion recovery imaging and its axial MIP reconstruction in multiple sclerosis. *Egyptian Journal of Radiology and Nuclear Medicine*, 53, Article 63. <https://doi.org/10.1186/s43055-022-00734-0>